Article

Synergistic Effect of Cu₂O and Urea as Modifiers of TiO₂ for Enhanced Visible Light Activity

Marcin Janczarek [1,2,*], Kunlei Wang [1] and Ewa Kowalska [1]

[1] Institute for Catalysis, Hokkaido University, N21, W10, Sapporo 001-0021, Japan;
kunlei@cat.hokudai.ac.jp (K.W.); kowalska@cat.hokudai.ac.jp (E.K.)

[2] Department of Chemical Technology, Gdansk University of Technology, Narutowicza Str. 11/12,
80-233 Gdansk, Poland

[*] Correspondence: mjancz@pg.edu.pl; Tel.: +48-58-3472352

Abstract: Low cost compounds, i.e., Cu₂O and urea, were used as TiO₂ modifiers to introduce visible light activity. Simple and cheap methods were applied to synthesize an efficient and stable nanocomposite photocatalytic material. First, the core-shell structure TiO₂–polytriazine derivatives were prepared. Thereafter, Cu₂O was added as the second semiconductor to form a dual heterojunction system. Enhanced visible light activity was found for the above-mentioned nanocomposite, confirming a synergistic effect of Cu₂O and urea (via polytriazine derivatives on titania surface). Two possible mechanisms of visible light activity of the considered material were proposed regarding the type II heterojunction and Z-scheme through the essential improvement of the charge separation effect.

1. Introduction

Titanium dioxide (TiO₂, titania) is widely recognized as an efficient, stable, and green photocatalytic material (long term stability, chemical inertness and corrosion resistance). Therefore, its application potential in photocatalysis is still growing and presently focuses on emergency areas, such as environmental remediation (water treatment and air purification), renewable energy processes (i.e., photocurrent generation, water splitting for hydrogen production, conversion of CO₂ to hydrocarbons) and self-cleaning surfaces [1–5]. However, the application of titania is still limited to regions with a high intensity of solar radiation due to its wide bandgap (ca. 3.0 to 3.2 eV). The following strategies of titania doping, modification, semiconductor coupling, and dye sensitization can be applied to incorporate visible light absorption to TiO₂ [6–8]. The nature of electron transfer between TiO₂ and other materials has been intensively studied and recognized as the origin of the high performances of TiO₂-based composites [9]. The photocatalytic activity of TiO₂ systems depend on the following properties, such as particle size, surface area, crystal phase, morphology, uncoordinated surface sites, defects in the lattice, and degree of crystallinity. Design of TiO₂ composite structures based on the heterojunction between titania and other semiconducting materials can improve many of these properties. Moreover, this strategy can create and tune other properties, such as mid-band-gap electronic states, which can be responsible for the intensification of charge separation or incorporation of a red shift to the absorption spectrum [7,9].

Copper oxides (Cu₂O, CuO) have been intensively studied as titania modifiers due to their intrinsic p-type configuration. Cu₂O and CuO are inexpensive semiconductors with band gap energies of 2.1–2.2 eV and 1.2–1.7 eV, respectively. This fact makes both materials promising for research directed to solar energy utilization [10–12]. If the electronic properties of both oxides are

compared, CuO has a significantly smaller band gap than Cu_2O, and thus can absorb more photons, but the positions of CB and VB for CuO are insufficient to catalyze the generation of hydroxyl and superoxide radicals, which are the primary initiators for the photocatalytic oxidation of organic compounds [13,14]. Therefore, the photocatalytic oxidation of organic compounds over Cu_2O/TiO_2 composites has been of particular interest, especially to introduce visible light activity to TiO_2-based systems [15–19]. For example, Liu et al. prepared Cu_2O/TiO_2 composites where titania was in the form of nanosheets with exposed {001} facets. They reported visible light photocatalytic activity for Cu_2O/TiO_2 nanosheets three times higher than that for nitrogen-doped titania nanosheets. Owing to the type II heterojunction between Cu_2O and TiO_2, an efficient charge separation is observed and visible light induced electron transfer from Cu_2O to TiO_2 occurs, resulting in visible light photocatalytic performance of the system [17]. Furthermore, Cu_2O possesses promising application potential because of its very good antipathogenic properties, even better than that of metallic copper [20–23].

Apart from p-type semiconducting metal oxides as composite junctions for titania, a promising option to prepare efficient and low cost visible light-active material based on TiO_2 is the application of organic compounds like urea as a modifier. Urea-derived titania materials were initially recognized as nitrogen "doped" TiO_2 photocatalysts [24–27]. Subsequently, the presence of nitridic and amidic species or nitrogen species with several oxidation states of nitrogen were suggested [25,26]. Finally, Mitoraj and Kisch proposed another explanation for the nature of urea-modification of titania including both nitrogen and carbon originating from urea as the elements building the chemical structure responsible for visible light-sensitization of TiO_2 [28–30]. They reported that thermal processing of urea with titania at 400 °C produced poly(amino-tri-*s*-triazine) derivatives (shell) covalently attached to the semiconductor (core), i.e., a unique example of inorganic with an organic (polytriazine as a crystalline layer) semiconductor connected through the Ti–N–C bond. Titania acts as a catalyst in this urea transformation. Condensation between the triazine amino and titania hydroxy groups forms Ti–N bonds. Considered chemical structures arise from condensed aromatic *s*-triazine compounds containing melem and melon (trimer of melem) units, which form a visible light absorbing semiconducting organic layer coupled with titania. Compared to unmodified TiO_2, the prepared photocatalyst may exhibit a band-gap narrowing. It has been proposed that the absorption shoulder in the visible region corresponding to this material is a charge-transfer band enabling an optical transfer from polytriazine component to titania [29]. In contrast, it is known that prolonged heating of urea at 550 °C produces polycondensed *s*-triazines with a graphitic structure (*g*-C_3N_4), which was recognized as a separate metal-free polymeric n-type semiconductor (band gap energy equal to 2.7 eV) with the possibility to create heterojunctions with other semiconductors, e.g., titania [31–34]. Therefore, thermal treatment of a TiO_2/urea composite at higher temperature results in the formation of a TiO_2/g-C_3N_4 heterojunction, whereas at lower temperatures, novel electronic states responsible for visible light activity located near valence band of titania originating from the presence of poly(amino-*s*-triazine) shell are formed [6].

Herein, we demonstrate that titania with a polytriazine layer originated from urea, and modified with Cu_2O ($Cu_2O/PTr–TiO_2$) becomes an efficient visible light photocatalyst, significantly more active than that of single modified titania, i.e., $PTr–TiO_2$ or Cu_2O/TiO_2. The preparation method is economically and practically attractive by using low cost components such as urea and Cu_2O and simple synthetic operations, i.e., lower temperatures of preparation in comparison with *g*-C_3N_4 synthesis (400 v. 550 °C). The important issue is the probable proposition of the explanation of the synergistic behavior of two different modifiers with corresponding visible light activation mechanisms. There are only two studies describing combinations of *g*-C_3N_4 with Cu_2O [35] and additionally with TiO_2 [36] showing improvements of visible light photocatalytic activity in comparison to single components (However, dyes have been used as test compounds, and thus origin of visible activity could not be unequivocally decided, i.e., dye sensitization could not be excluded [37,38]). Moreover, polycondensed *s*-triazines of graphitic structure were used, but not the non-graphitic forms obtained

at lower temperature as proposed by Mitoraj and Kisch [29]. To the best of our knowledge, this report is the first study for this type of photocatalytic material.

2. Results and Discussion

2.1. Preparation Conditions and Visible Light Photocatalytic Efficiency

Commercially available P25 titania was used as a base to prepare the final photocatalytic material ($Cu_2O/PTr–TiO_2$). The first step of preparation was to obtain $PTr–TiO_2$ with urea as a modifier (preparation details in Materials and Methods). "PTr" symbolizes the polytriazine shell. Different ratios between urea and P25 were investigated: 0.5:1, 1:1, 2:1 and 3:1 to find the material with the best photocatalytic efficiency under visible light irradiation. Samples with different shades of yellow color were obtained (more intensive yellow represents a higher amount of urea). 2-propanol oxidation to acetone was selected as the reaction system to test visible light photocatalytic activity ($\lambda > 455$ nm). The sample prepared at 1:1 urea–P25 ratio possessed the highest photocatalytic activity (measured as the produced acetone amount) and was chosen for further research and marked as $PTr–TiO_2$ (see Figure 1). It was found that higher amounts of urea were not advantageous for the photocatalytic activity of the final product probably due to the detrimental influence of some not converted products of urea thermal transformation (excess of urea) on the semiconducting character of the polytriazine shell structure, as previously reported [29].
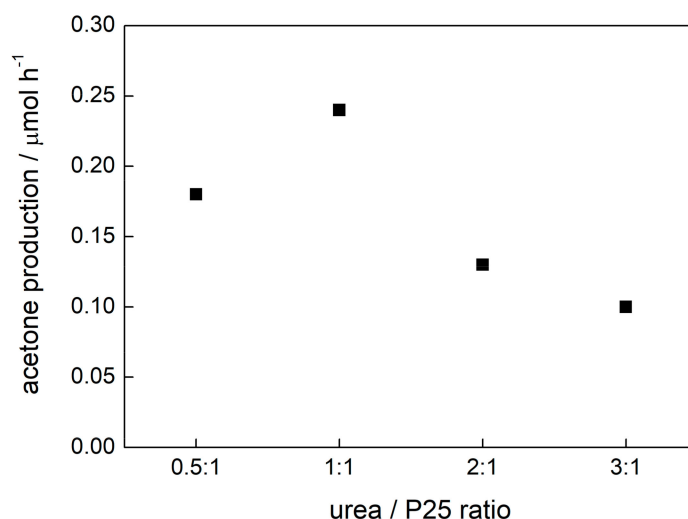

Figure 1. Visible light photocatalytic activity of the samples prepared with corresponding urea/P25 ratio.

The second step in the photocatalyst preparation was the physical mixing of $PTr–TiO_2$ with Cu_2O by using different contents of Cu_2O. Figure 2 shows the evidence of the advantageous role of the addition of cuprous oxide to the $PTr–TiO_2$ sample. The optimum Cu_2O content was found to be in the range of ca. 5 wt %, whereas 10 wt % and larger amounts were detrimental for photocatalytic efficiency. Detrimental influence of modifiers at their larger contents on photocatalytic activity is not surprising, and has already been reported for various systems. There are two main reasons for this behavior, i.e., (i) a shielding effect as Cu_2O blocks $PTr–TiO_2$ for photon absorption; and (ii) competitive adsorption as the oxygen and/or organic compounds (here 2-propanol) could not adsorbed directly on the titania surface, occupied by its modifier. Based on the obtained results, 5 wt % was chosen the Cu_2O content in the $Cu_2O/PTr–TiO_2$ sample.
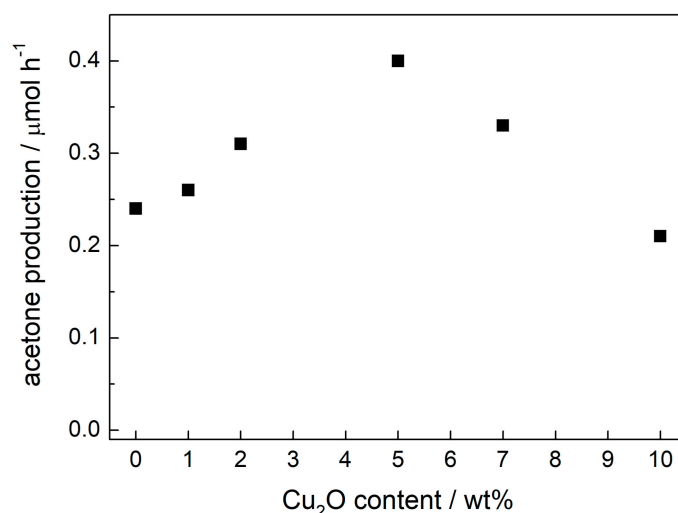
Figure 2. Visible light photocatalytic activity of the samples prepared with different Cu_2O content.

2.2. Characterization of Samples

P25 is a well-known mixed-phase titania photocatalyst containing two crystalline phases: anatase (86.4%) and rutile (13.6%), and amorphous titania (exact composition using NiO as the internal standard was estimated previously showing the anatase/rutile/amorphous ratio to be 76–80/13–15/6–11 (P25 is not a uniform sample) [39]) with a 21 nm crystallite size of anatase (determined from XRD) and 59.1 m^2/g specific surface area. After the thermal treatment with urea, the properties of the PTr–TiO_2 sample (1:1 urea–P25 ratio) changed slightly to a 23 nm crystallite size of anatase and 62.3 m^2 g^{-1} specific surface area, but the crystalline phase content remained unchanged. It is proposed that an increase in crystallite size should result from amorphous titania conversion to anatase during calcination, whereas an increase in specific surface area comes from the adsorbed organic layer of poly(amino-tri-*s*-triazine) derivatives. Cu_2O, which was used as a component of the Cu_2O–PTr–TiO_2 mixture, was characterized by a 65 nm crystallite size and 23 m^2 g^{-1} specific surface area. Therefore, the results stated that the PTr–TiO_2 crystallites were almost three times smaller than the Cu_2O ones. These values were confirmed by XRD analysis of the Cu_2O/PTr–TiO_2 sample. Figure 3 shows the XRD diffractogram of Cu_2O/PTr–TiO_2 with peaks corresponding to anatase, rutile, and Cu_2O. An aromatic system of carbon nitrides should appear at around 27.4°, but a strong peak of rutile overlaps it. It was reported that in the case of a small fraction of polycondensed polytriazines, this peak would not be detected [29].
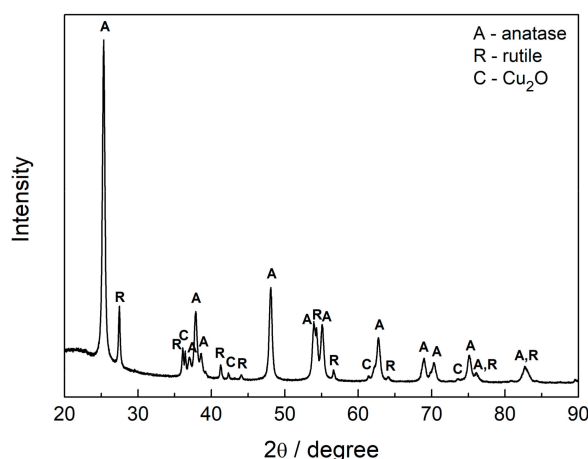

Figure 3. XRD diffractogram of Cu_2O/PTr–TiO_2 sample.

The diffuse reflectance spectra of the PTr–TiO$_2$ and Cu$_2$O/PTr–TiO$_2$ samples (Figure 4) show the strong red shift originated from the absorption properties of the polytriazine layer on P25. The visible light absorption effect was stronger than that for similar samples reported by Mitoraj and Kisch [28,30]. However, a different type of titania was used as the base for synthesis in that study. Therefore, it was proposed that the content of the surface hydroxyl groups on the surfaces of the various TiO$_2$ samples were responsible for better/worse ability of polytriazine layer formation (the issue of finishing the process of formation polytriazine layer by the reaction of amino groups of the relevant intermediates with titania surface OH groups [30]). To check this hypothesis, reference experiments were performed for own-prepared decahedral anatase particles (DAP) [40] modified with urea using the same conditions as for P25. Interestingly, it was observed that the DAP sample after this modification practically did not change, i.e., the color was still white and the visible light activity was not observed. Accordingly, it is proposed that the highly crystalline titania samples with low surface area (DAP as an example) possess too low number of surface OH groups to successfully introduce the polytriazine layer on their surfaces. It is also possible that surface defects, e.g., oxygen vacancy, play a crucial role in polytriazine layer formation since the DAP (well-crystallized faceted titania) possess an extremely low content of such defects (clarification of this phenomenon for other titania samples is under study). Mitoraj and Kisch proposed that the visible light absorption of urea-modified samples with a yellow color originated from the presence of poly(tri-*s*-triazine) centered intra-bandgap levels which may form (depending on PTr concentration) a narrow energy band in titania [29]. Additionally, in the case of the Cu$_2$O/PTr–TiO$_2$ photocatalyst, more intensive light absorption in the range 450–600 nm, as the consequence of the inherent light absorption properties of Cu$_2$O, was observed (Figure 3). The Cu$_2$O/PTr–TiO$_2$ sample had a reddish-yellow color.
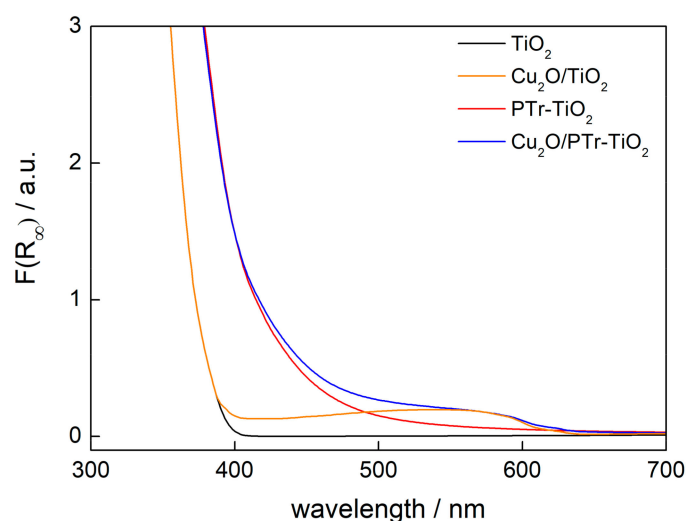

Figure 4. Diffuse reflectance spectra of TiO$_2$, PTr–TiO$_2$, Cu$_2$O/PTr–TiO$_2$. The Kubelka–Munk function F(R$_\infty$) is equivalent to absorbance.

XPS analysis of PTr–TiO$_2$ and Cu$_2$O/PTr–TiO$_2$ samples showed the presence of nitrogen 1s with binding energies of 399.1 and 400.5 eV, which indicates the presence of C=N–C and (–C=N–)$_x$ bonds, respectively, being in agreement with previously reported values [29,41,42]. XPS results showing the fractions of oxidation states of titanium, oxygen and copper are shown in Table 1. For samples modified with urea (PTr–TiO$_2$ and Cu$_2$O/PTr–TiO$_2$), the content of oxygen related to hydroxyl groups bound to titanium and carbon was lower than for bare TiO$_2$ due to the fact that surface hydroxyl groups participate in poly-*s*-triazine layer formation. In contrast, the content of Ti^{3+} increased after modification, which could confirm the participation of surface defects in the formation of PTr–TiO$_2$ (as discussed above for modified faceted titania (DAP)). It is proposed that thermal treatment could increase the formation of Ti^{3+}.

Therefore, it is also possible that a decrease in the content of hydroxyl groups after titania modification could result from their replacement by poly-*s*-triazine, similar to titania surface modification with nanoparticles of noble metals [43]. Moreover, samples with the poly-*s*-triazine layer also had a higher carbon content (higher C/Ti ratio). These results confirmed the presence of an organic layer on the titania surface consisting of poly-*s*-triazine derivatives, as reported previously [29].

Table 1. XPS analysis for TiO_2, $PTr–TiO_2$ and $Cu_2O/PTR–TiO_2$ samples including fraction of oxidation states of Ti, O, and Cu from the deconvolution of XPS peaks of Ti $2p_{3/2}$, O 1s and Cu $2p_{3/2}$.

Samples	Ti $2p_{3/2}$ (%)		O 1s (%)			Ratio		Valent State (%)		
	Ti^{4+}	Ti^{3+}	TiO_2 [a]	Ti-OH [b]	Ti-OH [c]	O/Ti	C/Ti	Cu^{2+}	Cu$^+$	Cu(0)
TiO_2	98.5	1.5	57.9	26.7	15.4	2.6	3.5	–	–	–
PTr-TiO_2	97.2	2.8	62.3	23.7	14.0	2.5	4.1	–	–	–
$Cu_2O/PTr-TiO_2$	97.0	3.0	61.8	24.1	14.1	2.5	4.3	0.9	99.1	–

[a] Oxygen in the TiO_2 crystal lattice; [b] Ti–(OH)–Ti, Ti_2O_3, C=O; [c] Ti–OH, C–OH.

To confirm the presence of the organic layer and possible formation of the $Cu_2O/PTr–TiO_2$ heterojunction, scanning transmission electron microscopy (STEM) observation was carried out. It was found that Cu_2O existed in both crystalline and amorphous forms (large aggregates of very fine NPs). Moreover, two kinds of crystalline structures were noticed, i.e., large crystals of 100–150 nm and fine faceted nanocrystals of 10–30 nm (cubic and decahedral). For the $Cu_2O/PTr-TiO_2$ sample, titania particles were covered with a 5–10-nm layer of polytriazine located nearby larger Cu_2O crystallites, as clearly shown in Figure 5 (respective SEM and TEM modes of the same image). Moreover, fine amorphous Cu_2O interconnecting $PTr–TiO_2$ particles was also observed. Interestingly, it was found that long-term electron beam during STEM observations could destroy the polytriazine layer around the titania since new nanostructures were formed (gravitationally-formed honey-like tails).
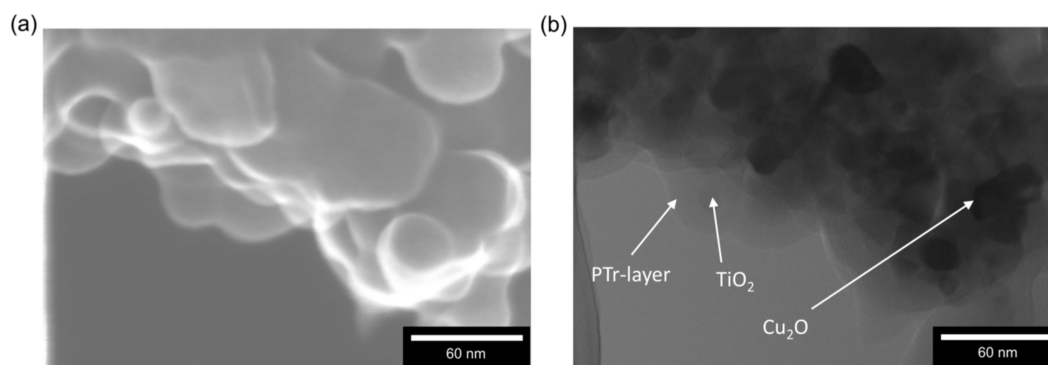

Figure 5. STEM images of $Cu_2O/PTr–TiO_2$ sample in SEM (**a**) and TEM (**b**) modes.

2.3. Enhanced Visible Light Photocatalytic Activity as a Synergistic Effect of Two Modifiers

Figure 6 shows the results of the photocatalytic activity tests of five photocatalysts: TiO_2, Cu_2O, Cu_2O/TiO_2, PTr-TiO_2, and $Cu_2O/PTr–TiO_2$ in the visible light-induced 2-propanol oxidation. The highest activity was observed for $Cu_2O/PTr-TiO_2$ with 1.2 μmol of acetone formation after 3 h of irradiation. The Cu_2O/TiO_2 and $PTr–TiO_2$ samples were characterized by significantly lower photoactivity: 0.18 and 0.72 μmol of acetone, respectively. The unmodified photocatalysts TiO_2 (P25) and Cu_2O were almost inactive in this reaction system. The improvement of visible light photocatalytic performance for the $Cu_2O/PTr–TiO_2$ sample in comparison to the Cu_2O/TiO_2 and $PTr–TiO_2$ photocatalysts is evidence of the synergistic effect of urea (poly(tri-*s*-triazine)) and Cu_2O modifiers for enhancing the visible light photocatalytic activity of titania. The photocatalytic activity test for the $Cu_2O/PTr–TiO_2$ sample was extended to 8 h to check the basic stability of the material. After 8 h of irradiation, a linear course of acetone production was still observed.
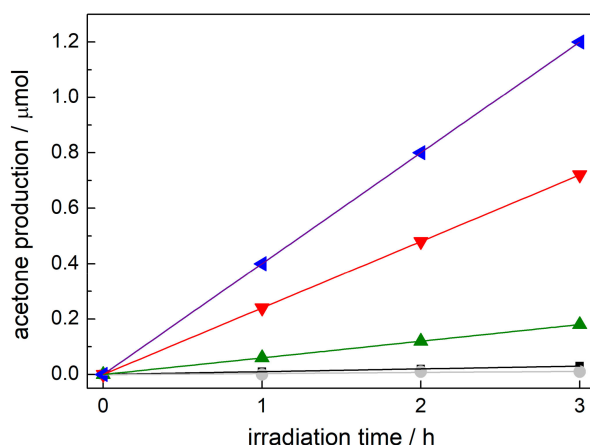
Figure 6. Visible light-induced ($\lambda > 455$ nm) 2-propanol oxidation in the presence of (■) TiO_2, (●) Cu_2O, (▲) Cu_2O/TiO_2, (▼) PTr-TiO_2, and (◄) Cu_2O/PTr-TiO_2.

A lack of visible light activity for a single Cu_2O, in spite of its good visible light absorption properties, can be explained by a strong photocorrosion effect and fast charge recombination [44,45]. It was reported that the coupling of cuprous oxide with titania reduced these detrimental effects by the heterojunction mechanism (type II) between the p- and n-type semiconductors introducing visible light activity and enhancing stability [15–19,46].

The PTr–TiO_2 photocatalyst possesses significantly higher visible light activity for 2-propanol oxidation than Cu_2O/TiO_2. The core-shell structure of titania–poly(tri-*s*-triazine) derivatives changes photoabsorption and electronic properties in comparison to the unmodified titania. Figure 7 shows a way to determine band gap energy and absorption onset for the PTr–TiO_2 sample. The band gap narrowing occurred from 3.17 eV for bare TiO_2 (P25) to 2.88 eV for PTr-TiO_2. The absorption onset is useful to determine the location of surface states in PTr–TiO_2 originating from the presence of an organic modifier (shaded area in the Figures 8 and 9) [6].
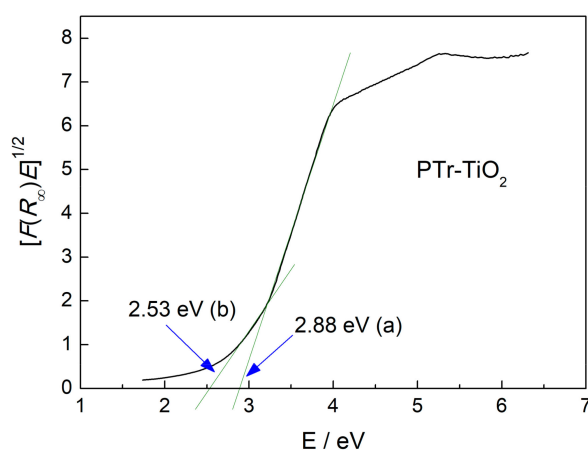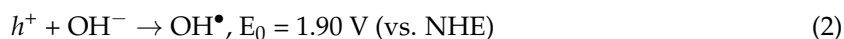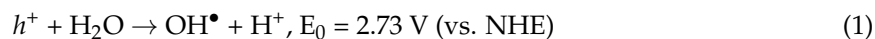

Figure 7. Plot of transformed Kubelka–Munk function vs. energy of light for the PTr–TiO_2 sample. Determination of band gap energy (**a**) and absorption onset (**b**).

Figures 8 and 9 illustrate the propositions of explanation for enhanced visible light photocatalytic activity of Cu_2O/PTr–TiO_2, a photocatalytic system with two main composites. In the first mechanistic variant (Figure 7), two semiconductors: p-type Cu_2O and n-type titania (P25) with an organic sensitizer created a type II heterojunction. This system provided the optimum band positions for efficient charge carrier separation. Visible light photoexcited electrons were transferred from $CB(Cu_2O)$ to

CB(PTr–TiO$_2$) and this transfer could occur due to the favorable energetics of the relative positions of both CBs, whereas holes were simultaneously transferred from VB(PTr–TiO$_2$) to VB(Cu$_2$O). The main consequence of such phenomenon is the separation of the photogenerated electrons and holes reducing the probability of recombination and increasing the lifetimes of the charge carriers [46]. Cu$_2$O has a valence band potential of 1.07 V [47]. To form hydroxyl radicals, the valence band potential of Cu$_2$O should be more positive than the following values at pH = 7 [7]:

$$h^+ + H_2O \rightarrow OH^\bullet + H^+, \; E_0 = 2.73 \text{ V (vs. NHE)} \qquad (1)$$

$$h^+ + OH^- \rightarrow OH^\bullet, \; E_0 = 1.90 \text{ V (vs. NHE)} \qquad (2)$$

Therefore, the formation of hydroxyl radicals may be thermodynamically unfavorable. It can be concluded that holes accumulated would be mostly consumed through the direct oxidation of 2-propanol. Electrons accumulated on CB(PTr–TiO$_2$) play a key role in the formation of reactive oxygen species. The properties of the PTr–TiO$_2$ component of the considered semiconductor composition by introduction of visible light activity into titania enabled the formation of this advantageous heterojunction functioning under visible light irradiation.
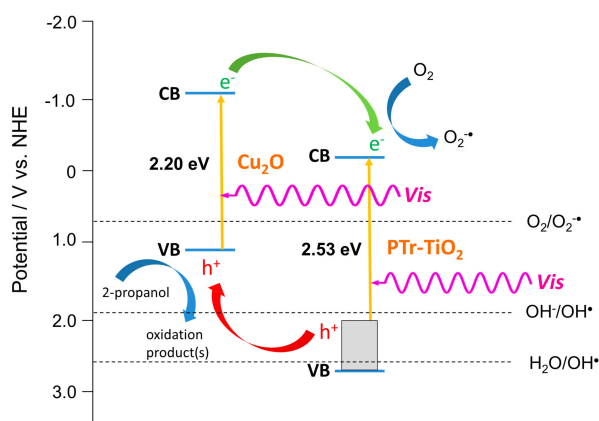

Figure 8. Energy diagram for the Cu$_2$O/PTr–TiO$_2$ photocatalytic system working under visible light, illustrating the coupling of two semiconductors as a type II heterojunction.
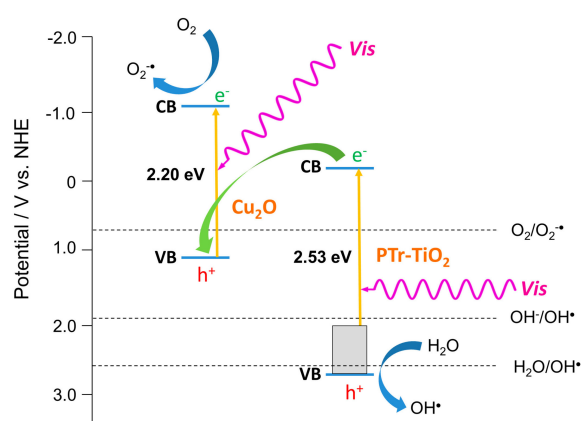

Figure 9. Energy diagram for Cu$_2$O/PTr–TiO$_2$ photocatalytic system working under visible light, illustrating the coupling of two semiconductors as a Z-scheme system.

Another mechanistic variant describing enhanced visible light activated Cu$_2$O/PTr–TiO$_2$ system relies on the Z-scheme concept [48,49]. As shown in Figure 9, photogenerated electrons in PTr–TiO$_2$

with a lower reduction ability recombined with the photogenerated holes in Cu_2O with lower oxidation ability. Therefore, electrons accumulated on $CB(Cu_2O)$ with a high reduction ability of holes accumulated on $VB(PTr–TiO_2)$ with a high oxidation ability can be maintained. The occurrence of the second mechanistic variant might be even more possible due to the existence of optimal Cu_2O content (Figure 2) and the low photocatalytic activity of the Cu_2O/TiO_2 system.

In the case of both mechanisms, the efficient charge separation induced by visible light irradiation was the main reason of the exceptional photocatalytic activity of the proposed system and provides the explanation of the synergistic role of the two considered types of titania modifiers. Clarification of which mechanistic variant is responsible for enhanced photocatalytic properties of the $Cu_2O/PTr–TiO_2$ system in the visible light is necessary. Further studies including action spectrum analysis, photoactivity tests in the presence of scavengers, and detailed characterization of these materials (and other photocatalysts prepared with different titania photocatalysts, i.e., varied by surface properties and/or content of oxygen defects), such as the estimation of the quasi–Fermi level, are along this line.

3. Materials and Methods

3.1. Preparation of $Cu_2O/PTr–TiO_2$

P25 (AEROXIDE® TiO_2 P25, Nippon Aerosil, Tokyo, Japan), urea (Wako Pure Chemicals, Osaka, Japan) and Cu_2O (Wako Pure Chemicals) were used for the study without purification. $PTr–TiO_2$ samples were prepared by the method based on the processes reported elsewhere [26,29]. Typically, 400 g of P25 powder and different amounts of urea corresponding to 0.5:1, 1:1, 2:1 and 3:1 (w/w) ratios were ground in an agate mortar, followed by calcination in air at 400 °C for 30 min. Powders were placed in the open test-tube with 15 cm of length. The resulting powders were washed five times with water to remove the excess of urea decomposition products and finally dried under air at 70 °C. In the second step, $PTr–TiO_2$ sample and Cu_2O powder (in different amounts: 1, 2, 5, 7, 10 wt %) were mixed thoroughly with 5 min of grinding.

3.2. Sample Characterization

The UV–Vis diffuse reflectance spectra (DRS) were recorded on JASCO V-670 (JASCO, Tokyo, Japan) equipped with PIN-757 integrating sphere using $BaSO_4$ as a reference. Gas-adsorption measurements of prepared titania samples were performed on a Yuasa Ionics Autosorb, 6AG (Yuasa Ionics, Osaka, Japan) surface area and pore size analyzer. Specific surface area (SSA) was calculated from nitrogen adsorption at 77 K using the Brunauer–Emmett–Teller equation. X-ray diffraction patterns (XRD) were collected using an X-ray diffractometer (Rigaku intelligent XRD SmartLab with a Cu target, Rigaku, Tokyo, Japan). X-ray photoelectron spectra (XPS) were recorded using a JEOL JPC-9010MC (JEOL, Tokyo, Japan) spectrometer with a MgKa X-ray source. Samples were also characterized by scanning transmission electron microscopy (STEM, HITACHI HD-2000, HITACHI, Tokyo, Japan).

3.3. Photocatalytic Reaction

The photocatalyst (50 mg) was suspended in an aqueous solution of 2-propanol (5 vol %, 5 mL) and photoirradiated (120 W-xenon lamp) with a Y48 cut-off filter mounted in the irradiation window, therefore the light of wavelengths >450 nm reached the suspension, which was under continuous magnetic stirring (1000 rpm) in a thermostated bath. Generated acetone was detected using GC–FID (Shimadzu GC-14B (Shimadzu, Kyoto, Japan) equipped with a flame ionization detector). Before the injection of the liquid sample to GC, the photocatalyst was separated using a filter (Whatman Mini-UniPrep, PVDF, Whatman, Maidstone, UK).

4. Conclusions

The results presented in this study clearly revealed that the application of both low cost- modifiers for titania: urea (first step of preparation) and Cu_2O (second step), significantly enhanced the visible light photocatalytic properties of TiO_2 in comparison to the single materials of urea-modified TiO_2 and Cu_2O-modified titania. Therefore, it is possible to describe this phenomenon as a synergistic effect of urea (more detailed: the presence of polytriazine layer on titania originated from the thermal treatment of urea) and Cu_2O. The type II heterojunction or Z-scheme systems formed by two semiconductors, p-type Cu_2O and n-type PTr–TiO_2, can be responsible for the improvement of photocatalytic activity through the intensification of visible light-induced charge separation and subsequent reduction of the electron-hole recombination effect. A preparation of composite photocatalysts based on titania and low-cost materials as modifiers, such as a precursor of the organic sensitizer of titania and metal oxide, to prepare the efficient and stable photocatalytic system operating in the visible light within heterojunction principles is a very promising direction for a wider practical application of photocatalysis given the preference for concomitantly cheap and efficient solutions.

References

1. Bahnemann, D.W. Photocatalytic water treatment: Solar energy applications. *Solar Energy* **2004**, *77*, 445–459. [CrossRef]
2. Chen, X.B.; Shen, S.H.; Guo, L.J.; Mao, S.S. Semiconductor-based photocatalytic hydrogen generation. *Chem. Rev.* **2010**, *110*, 6503–6570. [CrossRef] [PubMed]
3. Li, K.; Peng, B.S.; Peng, T.Y. Recent advances in heterogeneous photocatalytic CO_2 conversion to solar fuels. *ACS Catal.* **2016**, *6*, 7485–7527. [CrossRef]
4. Pietron, J.J.; DeSario, P.A. Review of roles for photonic crystals in solar fuels photocatalysis. *J. Photonics Energy* **2016**, *7*, 012007. [CrossRef]
5. Ragesh, P.; Ganesh, V.A.; Nair, S.V.; Nair, A.S. A review on 'self-cleaning and multifunctional materials'. *J. Mater. Chem. A* **2014**, *2*, 14773–14797. [CrossRef]
6. Kisch, H. Semiconductor photocatalysis—Mechanistic and synthetic aspects. *Angew. Chem. Int. Ed.* **2013**, *52*, 812–847. [CrossRef] [PubMed]
7. Schneider, J.; Matsuoka, M.; Takeuchi, M.; Zhang, J.; Horiuchi, Y.; Anpo, M.; Bahnemann, D.W. Understanding TiO_2 photocatalysis: Mechanisms and materials. *Chem. Rev.* **2014**, *114*, 9919–9986. [CrossRef] [PubMed]
8. Pelaez, M.; Nolan, N.T.; Pillai, S.C.; Seery, M.K.; Falaras, P.; Kontos, A.G.; Dunlop, P.S.M.; Hamilton, J.W.J.; Byrne, J.A.; O'Shea, K.; et al. A review on the visible light active titanium dioxide photocatalysts for environmental applications. *Appl. Catal. B Environ.* **2012**, *125*, 331–349. [CrossRef]
9. Dahl, M.; Liu, Y.; Yin, Y. Composite titanium dioxide nanomaterials. *Chem. Rev.* **2014**, *114*, 9853–9889. [CrossRef] [PubMed]
10. Bhanushali, S.; Ghosh, P.; Ganesh, A.; Cheng, W.L. 1D copper nanostructures: Progress, challenges and opportunities. *Small* **2015**, *11*, 1232–1252. [CrossRef] [PubMed]
11. Clarizia, L.; Spasiano, D.; Di Somma, I.; Marotta, R.; Andreozzi, R.; Dionysiou, D.D. Copper modified-TiO_2 catalysts for hydrogen generation through photoreforming of organics. A short review. *Int. J. Hydrogen Energy* **2014**, *39*, 16812–16831. [CrossRef]
12. Janczarek, M.; Kowalska, E. On the origin of enhanced photocatalytic activity of copper-modified titania in the oxidative reaction systems. *Catalysts* **2017**, *7*, 317. [CrossRef]

13. Nguyen, M.A.; Bedford, N.M.; Ren, Y.; Zahran, E.M.; Goodin, R.C.; Chagani, F.F.; Bachas, L.G.; Knecht, M.R. Direct Synthetic Control over the Size, Composition, and Photocatalytic Activity of Octahedral Copper Oxide Materials: Correlation Between Surface Structure and Catalytic Functionality. *ACS Appl. Mater. Interfaces* **2015**, *7*, 13238–13250. [CrossRef] [PubMed]

14. Deng, X.L.; Wang, C.G.; Shao, M.H.; Xu, X.J.; Huang, J.Z. Low-temperature solution synthesis of CuO/Cu_2O nanostructures for enhanced photocatalytic activity with added H_2O_2: Synergistic effect and mechanism insight. *RSC Adv.* **2017**, *7*, 4329–4338. [CrossRef]

15. Yang, L.; Luo, S.; Li, Y.; Xiao, Y.; Kang, Q.; Cai, Q. High efficient photocatalytic degradation of p-nitrophenol on a unique Cu_2O/TiO_2 p-n heterojunction network catalyst. *Environ. Sci. Technol.* **2010**, *44*, 7641–7646. [CrossRef] [PubMed]

16. Chu, S.; Zheng, X.M.; Kong, F.; Wu, G.H.; Luo, L.L.; Guo, Y.; Liu, H.L.; Wang, Y.; Yu, H.X.; Zou, Z.G. Architecture of $Cu_2O@TiO_2$ core-shell heterojunction and photodegradation for 4-nitrophenol under simulated sunlight irradiation. *Mater. Chem. Phys.* **2011**, *129*, 1184–1188. [CrossRef]

17. Liu, L.; Gu, X.; Sun, C.; Li, H.; Deng, Y.; Gao, F.; Dong, L. In situ loading of ultra-small Cu_2O particles on TiO_2 nanosheets to enhance the visible-light photoactivity. *Nanoscale* **2012**, *4*, 6351–6359. [CrossRef] [PubMed]

18. Liu, L.M.; Yang, W.Y.; Li, Q.; Gao, S.A.; Shang, J.K. Synthesis of Cu_2O nanospheres decorated with TiO_2 nanoislands, their enhanced photoactivity and stability under visible light illumination, and their post-illumination catalytic memory. *ACS Appl. Mater. Interfaces* **2014**, *6*, 5629–5639. [CrossRef] [PubMed]

19. Xiong, L.B.; Yang, F.; Yan, L.L.; Yan, N.N.; Yang, X.; Qiu, M.Q.; Yu, Y. Bifunctional photocatalysis of TiO_2/Cu_2O composite under visible light: Ti^{3+} in organic pollutant degradation and water splitting. *J. Phys. Chem. Solids.* **2011**, *72*, 1104–1109. [CrossRef]

20. Qiu, X.; Miyauchi, M.; Sunada, K.; Minoshima, M.; Liu, M.; Lu, Y.; Li, D.; Shimodaira, Y.; Hosogi, Y.; Kuroda, Y.; et al. Hybrid Cu_xO/TiO_2 nanocomposites as risk-reduction materials in indoor environments. *ACS Nano* **2012**, *6*, 1609–1618. [CrossRef] [PubMed]

21. Hans, M.; Erbe, A.; Mathews, S.; Chen, Y.; Solioz, M.; Mucklich, F. Role of copper oxides in contact killing of bacteria. *Langmuir* **2013**, *29*, 16160–16166. [CrossRef] [PubMed]

22. Duan, W.; Zheng, M.; Li, R.; Wang, Y. Morphology transformation of Cu_2O by adding TEOA and their antibacterial activity. *J. Nanopart. Res.* **2016**, *18*, 342. [CrossRef]

23. Lee, Y.J.; Kim, S.; Park, S.H.; Park, H.; Huh, Y.D. Morphology-dependent antibacterial activities of Cu_2O. *Mater. Lett.* **2011**, *65*, 818–820. [CrossRef]

24. Nosaka, Y.; Matsushita, M.; Nishino, J.; Nosaka, A.Y. Nitrogen-doped titanium dioxide photocatalysts for visible response prepared by using organic compounds. *Sci. Technol. Adv. Mater.* **2005**, *6*, 143–148. [CrossRef]

25. Bacsa, R.; Kiwi, J.; Ohno, T.; Albers, P.; Nadtochenko, V. Preparation, testing and characterization of doped TiO_2 active in the peroxidation of biomolecules under visible light. *J. Phys. Chem. B* **2005**, *109*, 5994–6003. [CrossRef] [PubMed]

26. Kisch, H.; Sakthivel, S.; Janczarek, M.; Mitoraj, D. A low-band gap, nitrogen-modified titania visible-light photocatalyst. *J. Phys. Chem. C* **2007**, *111*, 11445–11449. [CrossRef]

27. Beranek, R.; Neumann, B.; Sakthivel, S.; Janczarek, M.; Dittrich, T.; Tributsch, H.; Kisch, H. Exploring the electronic structure of nitrogen-modified TiO_2 photocatalysts through photocurrent and surface photovoltage studies. *Chem. Phys.* **2007**, *339*, 11–19. [CrossRef]

28. Mitoraj, D.; Kisch, H. The nature of nitrogen-modified titanium dioxide photocatalysts active in visible light. *Angew. Chem. Int. Ed.* **2008**, *47*, 9975–9978. [CrossRef] [PubMed]

29. Mitoraj, D.; Kisch, H. On the mechanism of urea-Induced titania modification. *Chem. Eur. J.* **2010**, *16*, 261–269. [CrossRef] [PubMed]

30. Mitoraj, D.; Kisch, H. Surface modified titania visible light photocatalyst powders. *Solid State Phenom.* **2010**, *162*, 49–75. [CrossRef]

31. Dong, G.; Zhang, Y.; Pan, Q.; Qiu, J. A fantastic graphitic carbon nitride ($g-C_3N_4$) material: Electronic structure, photocatalytic and photoelectronic properties. *J. Photochem. Photobiol. C Photochem. Rev.* **2014**, *20*, 33–50. [CrossRef]

32. Liu, J.; Zhang, T.; Wang, Z.; Dawson, G.; Chen, W. Simple pyrolysis of urea into graphitic carbon nitride with recyclable adsorption and photocatalytic activity. *J. Mater. Chem.* **2011**, *21*, 14398–14401. [CrossRef]

33. Lee, S.C.; Lintang, H.O.; Yuliati, L. A urea precursor to synthesize carbon nitride with mesoporosity for enhanced activity in the photocatalytic removal of phenol. *Chem. Asian J.* **2012**, *7*, 2139–2144. [CrossRef] [PubMed]

34. Senthil, R.A.; Theerthagiri, J.; Selvi, A.; Madhavan, J. Synthesis and characterization of low-cost g-C$_3$N$_4$/TiO$_2$ composite with enhanced photocatalytic performance under visible-light rradiation. *Opt. Mater.* **2017**, *64*, 533–539. [CrossRef]

35. Peng, B.; Zhang, S.; Yang, S.; Wang, H.; Yu, H.; Zhang, S.; Peng, F. Synthesis and characterization of g-C$_3$N4/Cu$_2$O composite catalyst with enhanced photocatalytic activity under visible light irradiation. *Mater. Res. Bull.* **2014**, *56*, 19–24. [CrossRef]

36. Min, Z.; Wang, X.; Li, Y.; Jiang, J.; Li, J.; Qian, D.; Li, J. A highly efficient visible-light-responding Cu$_2$O-TiO$_2$/g-C$_3$N$_4$ photocatalyst for instantaneous discolorations of organic dyes. *Mater. Lett.* **2017**, *193*, 18–21. [CrossRef]

37. Kisch, H.; Macyk, W. Visible-light photocatalysis by modified titania. *Chem. Phys. Chem.* **2002**, *3*, 399–400. [CrossRef]

38. Yan, X.; Ohno, T.; Nishijima, K.; Abe, R.; Ohtani, B. Is methylene blue an appropriate substrate for a photocatalytic activity test? A study with visible-light responsive titania. *Chem. Phys. Lett.* **2006**, *429*, 606–610. [CrossRef]

39. Wang, K.; Wei, Z.; Ohtani, B.; Kowalska, E. Interparticle electron transfer in methanol dehydrogenation on platinum-loaded titania particles prepared from P25. *Catal. Today* **2018**, *303*, 327–333. [CrossRef]

40. Janczarek, M.; Kowalska, E.; Ohtani, B. Decahedral-shaped anatase titania photocatalyst particles: Synthesis in a newly developed coaxial-flow gas-phase reactor. *Chem. Eng. J.* **2016**, *289*, 502–512. [CrossRef]

41. Dementjev, A.P.; de Graaf, A.; van den Sanden, M.C.M.; Maslakov, K.I.; Naumkin, A.V.; Serov, A.A. X-Ray photoelectron spectroscopy reference data for identification of the C$_3$N$_4$ phase in carbon–nitrogen films. *Diam. Relat. Mater.* **2000**, *9*, 1904–1907. [CrossRef]

42. Guo, X.; Xie, Y.; Wang, X.; Zhang, S.; Hou, T.; Lv, S. Synthesis of carbon nitride nanotubes with the C$_3$N$_4$ stoichiometry via a benzene-thermal process at low temperatures. *Chem. Commun.* **2004**, 26–27. [CrossRef] [PubMed]

43. Janczarek, M.; Wei, Z.; Endo, M.; Ohtani, B.; Kowalska, E. Silver- and copper-modified decahedral anatase titania particles as visible light-responsive plasmonic photocatalyst. *J. Photonics Energy* **2017**, *7*, 012008. [CrossRef]

44. Bessekhouad, Y.; Robert, D.; Weber, J.-V. Photocatalytic activity of Cu$_2$O/TiO$_2$, Bi$_2$O$_3$/TiO$_2$ and ZnMn$_2$O$_4$/TiO$_2$ heterojunctions. *Catal. Today* **2005**, *101*, 315–321. [CrossRef]

45. Huang, L.; Peng, F.; Yu, H.; Wang, H. Preparation of cuprous oxides with different sizes and their behaviors of adsorption, visible-light driven photocatalysis and photocorrosion. *Solid State Sci.* **2009**, *11*, 129–138. [CrossRef]

46. Marschall, R. Semiconductor Composites: Strategies for Enhancing Charge Carrier Separation to Improve Photocatalytic Activity. *Adv. Funct. Mater.* **2014**, *24*, 2421–2440. [CrossRef]

47. Luna, A.L.; Valenzuela, M.A.; Colbeau-Justin, C.; Vazquez, P.; Rodriguez, J.; Avendano, J.R.; Alfaro, S.; Tirado, S.; Garduno, A.; De la Rosa, J.M. Photocatalytic degradation of gallic acid over CuO–TiO$_2$ composites under UV/Vis LEDs irradiation. *Appl. Catal. A Gen.* **2016**, *521*, 140–148. [CrossRef]

48. Li, H.; Tu, W.; Zhou, Y.; Zou, Z. Z-scheme photocatalytic systems for promoting photocatalytic performance: Recent progress and future challenges. *Adv. Sci.* **2016**, *3*, 1500389. [CrossRef] [PubMed]

49. Low, J.; Jiang, C.; Cheng, B.; Wageh, S.; Al-Ghamdi, A.A.; Yu, J. A review of direct Z-scheme photocatalysts. *Small Methods* **2017**, *1*, 1700080. [CrossRef]